Environmental Engineering and Management Journal

May 2015, Vol.14, No. 5, 1097-1110
http://omicron.ch.tuiasi.ro/EEMJ/

"Gheorghe Asachi" Technical University of Iasi, Romania

DETERMINATION OF EQUILIBRIUM, KINETIC AND THERMODYNAMIC PARAMETERS OF ACID RED 88 ADSORPTION ONTO MONTMORILLONITIC CLAY

Sedef Dikmen[1*], Ahmet Gunay[2], Bahri Ersoy[3], Ibrahim Erol[4]

[1]Department of Physics, Anadolu University, Faculty of Science, 26470, Eskisehir, Turkey
[2]Istanbul Metropolitan Municipality, Waste Management Directorate, 34360, Sisli, Istanbul, Turkey
[3]Department of Mining Engineering, Afyon Kocatepe University, 03200, Afyonkarahisar, Turkey
[4]Department of Chemistry, Afyon Kocatepe University, 03200, Afyonkarahisar, Turkey

Abstract

The aim of this study is to evaluate adsorption kinetics, isotherms and thermodynamic parameters of anionic textile dye (Acid Red 88) onto montmorillonitic clay from aqueous solutions. The parameters of pH, initial dye concentrations, temperature, and the adsorbent dosage were investigated experimentally. Four kinetic models including pseudo-second order, pseudo-nth order, Bangham's equation and double exponential equation (DEE) were selected to follow the adsorption process. The dynamic data were fitted the DEE well and also followed the pseudo-nth order model. The adsorption data obtained were well described by the Langmuir isotherm model. The maximum adsorption capacity was found to be 588 mg/g at 20 ^{o}C. Thermodynamic parameters such as activation energy (E_a), Gibbs free energy (ΔG^0), enthalpy (ΔH^0) and entropy (ΔS^0) were also evaluated. The negative value of change in Gibbs free energy indicates that adsorption of AR88 on montmorillonitic clay is spontaneous. The anionic dye molecules can be adsorbed on montmorillonitic clay particles, even when their surface charge (or zeta potential) is negative. Interactions leading to adsorption of anionic dyes (AR88) onto the clay may cause from the following mechanisms: hydrogen bonding, electrostatic interaction, hydrophobic interaction, anion exchange and dye-dye interactions. The results show that montmorillonitic clay could be employed as low-cost material for the removal of acid dyes from textile effluents.

Key words: acid red 88, adsorption, isotherms, montmorillonitic clay, thermodynamics

Received: October, 2011; Revised final: May, 2012; Accepted: June, 2012

1. Introduction

Colored organic effluent is produced in the textile, paint, pulp, paper, plastic, leather, food, dye, printing, ink, pharmaceutical, cosmetic, and leather processing industries. Among these industries, effluents from the dyeing and finishing processes in the textile industry are highly colored, with a large amount of suspended organic solid, which are important sources of water pollution. These effluents are also carcinogenic and pose a major threat to aquatic living organisms. The presence of even very low concentrations of these effluents is highly visible and potentially inhibiting photosynthesis. Due to their chemical structure, these dyes color the water and make penetration of sunlight to the lower layers impossible, consequently affecting aquatic life (Kannan and Sundaram, 2001; Luis et al., 2014; Mondal et al., 2014; Ozcan et al., 2005; Vandevivere et al., 1998; Weng and Pan, 2007; Won et al., 2006).

The degradation of dye concentrations in wastewater using traditional methods can be a threat, such as coagulation, sedimentation, membrane filtration, ozonation, oxidation, electrochemical

[*] Author to whom all correspondence should be addressed: E-mail: sdikmen@anadolu.edu.tr, szdikmen@gmail.com; Phone: +90 222 335 05 85; Fax: +90 222 320 49 10

destruction, physical-chemical flocculation combined with flotation based on the use of activated carbon (Akar et al., 2008; Banat et al., 1996; Fu and Viraraghavan, 2001). However, these methods have certain disadvantages such as high operating cost, regeneration problem, formation hazardous by-products and high energy requirements. The adsorption process is commonly adopted for the treatment of textile effluents because of its effectiveness and versatility (Crini, 2006).

Although activated carbon seems to be an efficient adsorbent, it has high operation costs. For this reason, many researchers are being focused to search for alternative adsorbents, such as clays including bentonite (Eren, 2009; Ozcan et al., 2005; Ozcan and Ozcan, 2004), kaolinite (Ghosh and Bhattacharyya, 2002; Harris et al., 2001; Tehrani-Bagha et al., 2011), montmorillonite (El Mouzdahir et al., 2010; Wang et al., 2004), sepiolite (Alkan et al., 2004, 2005; Armagan et al., 2003; Eren et al., 2010; Ozcan et al., 2006), palygorskite (Al-Futaisi et al., 2007), clinoptilolite (Colar et al., 2012) and smectite (Ogawa et al., 1996), which are used as adsorbents for the removal of dyes from wastewater. Clay minerals have found to be a more interesting adsorbent for adsorption studies due to its low cost, high surface charges, and well lamellar structure, which makes it a potential adsorbent for the removal of dye molecules (Monash and Pugazhenthi, 2010).

Adsorption of organic molecules by the clays is primarily controlled by surface properties of the clay and chemical structure of the dye molecules. Natural clays exhibit a negative charge of structure which allows it to adsorb positively charged dyes but induce a low adsorption capacity for anionic dyes. Therefore, a number of studies were achieved cationic dye adsorption onto clays, but a limited number of studies have been devoted to anionic dye adsorption onto clay (Akar and Uysal, 2010; Errais et al., 2010; Karaoglu et al., 2010; Vimonses et al., 2009; Tabak et al., 2009).

The present study is to investigate the possibility of untreated montmorillonitic clay from Eskisehir region (Turkey) as an adsorbent for removal of an anionic acid dye, which is called Acid Red 88, from aqueous solution by adsorption method. The adsorption process was optimized by investigating pH, contact time, initial dye concentrations, temperature, and the adsorbent dosage. The kinetics of adsorption was analyzed by fitting pseudo-second order, pseudo-nth order, Bangham's equation and double exponential equation (DEE).

The experimental data were fitted into Langmuir, Freundlich, Tempkin and Dubinin-Radushkevich (D-R) equations to determine which isotherm models give the best correlation to experimental data. Furthermore, the thermodynamic parameters such as, Gibbs free energy (ΔG^0), enthalpy (ΔH^0) entropy (ΔS^0) and activation energy (E_a) were obtained and surface properties were determined to provide insights to the adsorption reactions and mechanism.

2. Materials and methods

2.1. Materials

The textile dye, AR88 was obtained from Sigma-Aldrich and used as the representative compound for the experiments in this study. Its chemical structure is illustrated in Fig. 1. Montmorillonitic clay was provided from Dolsan Co. Ltd. (Eskisehir, Turkey) and used as an adsorbent for all experiments. The desired pH of the solution was kept constant during conditioning by introducing appropriate amounts of HCl or NaOH.

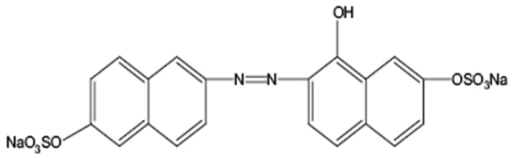

Fig. 1. The chemical structure of AR88

2.2. Material characterization

The mineralogy of the montmorillonitic clay was investigated by X-ray powder diffraction (XRD, Rigaku RINT 2200) obtained through the reference intensity ratio (RIR) procedure (Chipera and Bish, 2002). The chemical composition of the sample was determined with an X-ray fluorescence spectrometer (Bruker, S8 Tiger WDXRF). Prior to the chemical analysis, a 1.5 g sample and 7.5 g $Li_2B_4O_7$ were mixed in platinum crucibles, melted in a fusion device at 1300 ^oC, and formed as glass tablets.

The BET surface area of montmorillonitic clay was calculated from N_2 adsorption isotherm in the relative pressure range from 0.05 to 0.35 with a surface area analyzer (Quantachrome, Nova 2200). Also, the pore size distribution was analyzed with N_2 adsorption, following the BJH algorithm. The mesoporous volume was calculated less than a relative pressure of 0.95. True density analysis of montmorillonitic clay was carried out with a pycnometer (Quantachrome, Ultrapycnometer 1000).

Particle size distributions were measured by laser diffraction using a Mastersizer 2000 (Malvern Inst. Ltd., UK). The results were given in Table 1. A scanning electron microscope (SEM Leo-1430 VP) was employed to observe the morphology of the clay particles. Fourier transform infrared spectra (FTIR) of raw montmorillonitic clay, AR88, AR88-adsorbed montmorillonitic clay were recorded between 4000-400 cm^{-1} with a Perkin-Elmer BX-2 spectrophotometer by the KBr technique (the sample concentration was about 1 wt.%; a pure KBr disc was utilized as reference). Prior to FTIR analysis, dye adsorbed montmorillonitic clay were washed twice with distilled water and dried in an oven at 80 °C.

Table 1. Chemical composition and some physical properties of montmorillonitic clay

Chemical composition	
Constituents	Percentage
SiO_2	60.90
Al_2O_3	11.67
CaO	4.33
MgO	3.30
Fe_2O_3	0.79
K_2O	0.79
TiO_2	0.07
MnO	0.05
Others	0.10
LOI*	18.00
Total	100.00
Physical properties	
Specific surface area	74 m²/g
Pore size distribution	5-30 nm (avg. 14)
True density	2.33 g/cm^3
Particle size distribution	
• D90	30.71 µm
• D50 (average)	10.08 µm
• D10	2.81 µm

LOI: Loss on ignition

2.3. Dye adsorption experiments

Adsorption experiments with montmorillonitic clay were carried out by using the batch technique at 20, 30 and 40 ^{0}C. Effect of initial pH was investigated at various pH values. In the experiments, a 0.1 g adsorbent was added to each 50 mL of dye solution having an initial concentration of 750 mg/L and then the pH of the solution was adjusted between 2 and 11 by adding a small amount of dilute HCl or NaOH. The vials were shaken for 24 h on a thermostatic shaker and centrifuged at 10000 rpm for 2 min.

Effect of adsorbent dosage was investigated at 20 ºC. For the adsorbent dosage studies, 50mL of 750mg/L AR88 was added to each vial with different adsorbent amounts (0.05-0.55 g) at a constant pH. For kinetic studies, agitation speed of 140 rpm, adsorbent dosage of 2g/L, AR88 concentration of 750mg/L was kept constant. The suspensions were shaken for 24 h on a thermostatic shaker and centrifuged for 2 min at 10000 rpm at the end of each adsorption period. The dye concentration of each supernatant was measured with a UV-Vis spectrophotometer (Jenway) at the respective λ_{max} value, which is 505 nm for AR88.

The adsorbed amount of AR88 onto montmorillonitic clay was calculated by using the Eq. (1) taking into the concentration differences of the solution between the initial and remaining accounts, where q_e is the amount of dye adsorbed at equilibrium (mg/g), V is the volume of the solution (mL), m is the mass of the adsorbent used (g), C_0 and C_e are the initial and the equilibrium dye concentrations (mg/L).

$$q_e = \frac{(C_0 - C_e)V}{m} \qquad (1)$$

The validity of used kinetic models and adsorption models in this study can be quantitatively checked by using a normalized standard deviation **Δq (%)** calculated by the Eq. (2) following equation (Kapoor and Yang, 1989).

$$\Delta q\,(\%) = \sqrt{\frac{\sum[(q_{exp} - q_{cal}/q_{exp})]^2}{n-1}}\,100 \qquad (2)$$

2.4. Zeta potential measurements

The zeta potential of montmorillonitic clay were determined by a Zetasizer Nano ZS equipped with MPT-2 automatic titrator (Malvern Inst.) running by electrophoresis technique. The suspensions were conditioned under the adsorption testing conditions at 20 and 40 ^{o}C. A sample of 0.1 g in 50 mL of dye solution was shaken for 24 h.

The suspensions were kept still for 10 min to let larger particles settle at the same temperature. Approximately 10 mL of clear supernatant was removed from the adsorption test vial and placed in the electrophoretic cell. An adequate amount of the particle bed and introduced into the cell. Each data point is average of 10 measurements. On the other hand, zeta potential measurements were performed at different pH values in 10^{-3} M NaCl solution.

3. Results and discussion

3.1. Mineralogical and chemical composition of adsorbent

The adsorbent mainly consisted of montmorillonite (52.35 wt %) and cristobalite (27.51 wt %), with minor quantities of calcite (9.10 wt %); kaolinite (8.08 wt %) and quartz (3.95 wt %) (Fig. 2). Table 1 shows chemical analysis results of the major and some trace elements in the montmorillonitic clay sample.

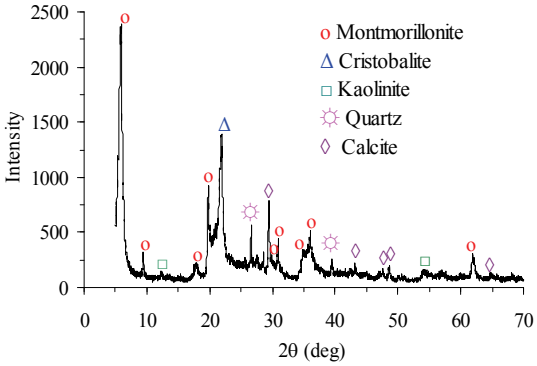

Fig. 2. X-ray diffraction pattern of montmorillonitic clay

The results indicate that SiO_2 and Al_2O_3 are the main components of the adsorbent, were 60.90% and 11.67%, respectively. The X-ray diffraction and chemical analysis of montmorillonitic clay indicate that cristobalite is the major impurities accompanying montmorillonite. Fig. 3 shows the

morphology of montmorillonitic clay that is characterized by typical layered particles.

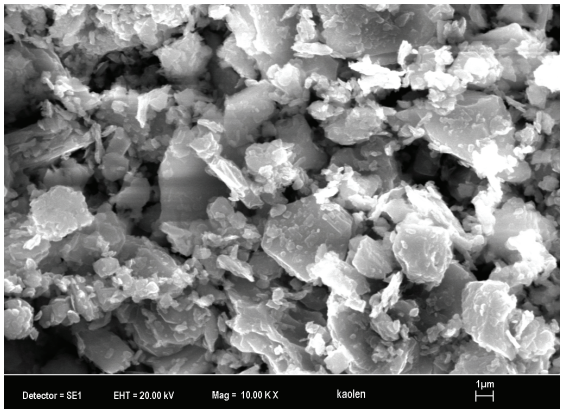

Fig. 3. SEM image of montmorillonitic clay

3.2. FTIR analysis

As indicated in the literature, the FTIR technique is used to identify the adsorption mechanisms of various organic compounds such as dye, surfactant, polymer etc (particularly those of physical, chemical, or hydrogen bonding) on various adsorbents like clay, fly ash etc. (Zaman et al., 2002; Acemioglu et al., 2004; Ozcan et al.,2005; Akyuz and Akyuz, 2006).

Accordingly, the FTIR spectroscopy is a useful tool in determining whether the adsorption interaction between montmorillonitic clay and AR88 is physical or chemical. The FTIR spectra of raw montmorillonitic clay, AR88, and the clay adsorbed with different amounts of AR88 are presented in Fig. 4.

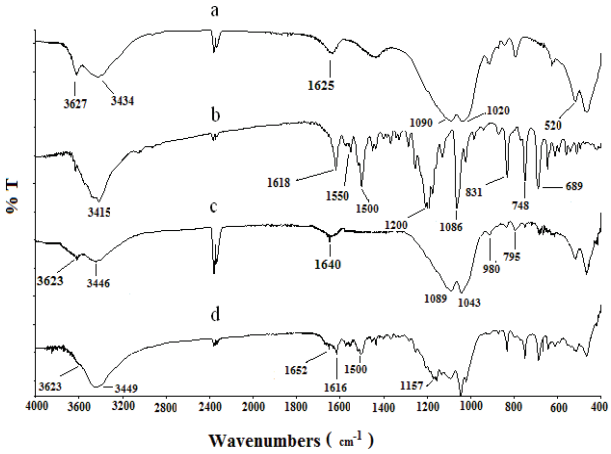

Fig. 4. FTIR spectra of (a) montmorillonitic clay, (b) anionic dye (AR88), (c) 225 mg/g and (d) 588 mg/g AR88-adsorbed montmorillonitic clay

There is a group of adsorption peaks between 3627 and 3434 cm^{-1}, which are due to stretching bands of the structural OH^- groups of montmorillonite, and the band at 1625 cm^{-1} also corresponds to the OH^- stretching of water molecules present in the clay (Fig. 4a) and dye adsorbed montmorillonitic clay (Fig. 4c-d), but the peak intensities of dye adsorbed-montmorillonitic clay are lower than that of raw montmorillonitic clay. The Si–O coordination band at 1090 cm^{-1} is observed as a result of the Si–O out-of-plane stretching vibration (Tyagi et al., 2006).

The band at around 1020 cm^{-1} represents the in-plane stretching of Si–O in the Si–O–Si groups of the tetrahedral sheet. The bands at 520 and 467 cm^{-1} are due to Si–O–Al (octahedral) and Si–O–Si bending vibrations, respectively (Tyagi et al., 2006; Akyuz and Akyuz, 2006). AR88 has the two most characteristic bands at 3415 cm^{-1} and 1618 cm^{-1} for OH^- and N=N groups (Fig. 4b). The aromatic C=C ring vibrations are shown at 1500 and 1550 cm^{-1}.

The C–O stretching is observed at 1165 and 1200 cm^{-1} and also the peaks at 1200 and 1086 cm^{-1} come from the stretching vibration of SO_3. The C–H in-plane bending and C=C out-of-plane bending vibrations of the aromatic nuclei are observed at 689 and 831 cm^{-1}, respectively (Gungor and Karaoglan, 2001; Wang et al., 1993). The FTIR spectra of the 225 and 588 mg/g AR88-adsorbed clay samples are given in Fig. 4c and 4d. Considerable differences are observed between the bands of montmorillonitic clay before and after dye adsorption, and also between the bands of free dye and those of adsorbed dye.

The stretching peak of OH^- group at 3434 cm^{-1} depending on clay shifted to approximately 3446 cm^{-1} after the adsorption and the intensity also increased. Similarly, the peak at 1625 cm^{-1} shifted to 1652 cm^{-1}. The OH^- peak of dye molecule at 3415 cm^{-1} shifted to approximately 3450 cm^{-1} after the adsorption of dye molecules. These variations in vibration frequencies are better observed as the dye adsorption increases.

These results indicate that the anionic dye molecules (AR88) can adsorb onto montmorillonitic clay, most likely through physical adsorption mechanisms such as H–bonding between the oxygen of the OH^- group of clay and the hydrogen of the OH^- group of AR88.

3.3. Effect of initial pH

The variations of both the zeta potentials of montmorillonitic clay particles and the amount adsorbed of the AR88 onto the clay with initial pH were investigated in the range of pH 2–11 and results are given Fig. 5. The adsorption of dye from aqueous solution onto surface of adsorbent is dependent on pH of the solution that affects the both nature of the surface charge of the adsorbent and speciation of the dye molecule. The adsorption capacity was 372 mg/g at initial pH of 2.4 and reduced to about 350 mg/g between at pH 7 and 8. Here, it should be noted that the natural pH of the suspension was approximately pH 8.5.

At lower pH more protons will be available, thereby increasing electrostatic attractions between negatively charged dye anions and positively charged adsorption sites and causing an increase in dye adsorption process.

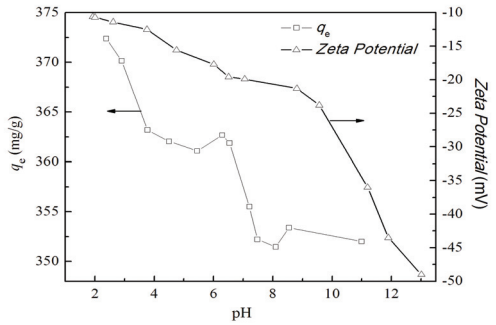

Fig. 5. The variation of both the amount adsorbed and zeta potential with initial pH of suspension. Conditions: C_0: 750 mg/L, adsorption temperature: 20 ºC, adsorption time: 24 h, agitation speed: 140 rpm, adsorbent dosage: 2 g/L

When the pH of the suspension is increased, the positive charge on the oxide or solution interfaces decreases and the clay surface appears negatively charged. On the contrary, a lower adsorption at higher pH may be due to the abundance of OH^- ions and because of ionic repulsion between the negatively charged surface and the ionic dye molecules.

There are also no exchangeable anions on the edge surface of clay at higher pH values and consequently the adsorption decreases (Ozcan and Ozcan, 2005). The curve of zeta potential versus pH also supported this finding. From Fig. 5, it can be seen that the adsorption capacity is the highest at pH 2.4 where the negative surface charge of particles is approximately –11 mV. Zeta potential decreases to –23 mV at natural pH and finally decreases to –43 mV approximately at pH 12. This decrease of zeta potential can be explained by the adsorption of OH^- ions bonded to the metal ions in the edge surface of the clay, and by the transport of H^+ ions into the water as a result of the ionization of OH^- groups bonded to metal.

While pH values affect the zeta potential of adsorbent, they do not show the same effect for dye adsorption capacity. Therefore, it may be said that the anionic dye molecule (AR88) can adsorb onto montmorillonitic clay particles even when their net surface potential is negative. A similar situation is also reported earlier for adsorption of anionic dyes onto negatively charged adsorbents (Alkan et al., 2004; Harris et al., 2001; Tunali et al., 2006).

3.4. Effect of adsorbent dosage

The effect of varying adsorbent dosage on AR88 adsorption was investigated at pH 9.6 and 20 ^{0}C.

The results were presented in Fig. 6. With an increase in the adsorbent dosage, from 1 and 4 g/L the percentage of AR88 removal increased from 58% to 97%, as the number of possible adsorbing sites would be increased, whereas the adsorption capacity of montmorillonitic clay for AR88 decreased from 521 to 61 mg/g.

Furthermore, the equilibrium concentration of AR88 sharply decreased adsorbent dosage ranging from 1 to 3 g/L, and then remained constant.

Consequently, the adsorbent dosage was determined as 2 g/L for further adsorption experiments.

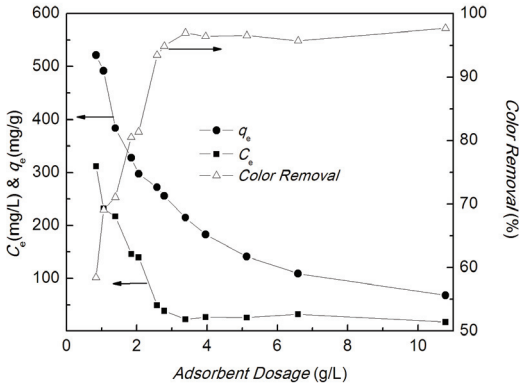

Fig. 6. The variation of both the amount adsorbed and color removal percentage with adsorbent dosage. Conditions: C_0: 750 mg/L, adsorption temperature: 20 ºC, adsorption time: 24 h, agitation speed: 140 rpm, equilibrium pH ≈ 9.6

3.5. Adsorption kinetics

The removal of AR88 by adsorption technique increased with time, reaching a maximum value at about 30-60 min, depending on initial concentration and temperature, thereafter it remained constant, as presented in Fig. 7a, b and c. These figures also compare the experimental and estimated q_e values for montmorillonitic clay. As can be seen from the data, double exponential equation (DEE) model provides the best fit to adsorbent/anionic dye (AR88) system for the whole contact time with higher correlation constant and lower standard deviations.

It is clearly seen from the figures that the agitation time required for maximum uptake (or to reach equilibrium) of AR88 by montmorillonitic clay was depended on the initial AR88 concentration. The adsorption rate of AR88 onto the clay was rapidly increased within 10 min, and then gradually decreased with increase in contact time. The kinetic study of the adsorption process provides useful information regarding the efficiency of adsorption and feasibility of scale-up operations.

Four kinetic models, i.e. pseudo-second order, pseudo-n^{th} order, Bangham's equation and double exponential equation (DEE), were considered to interpret the time dependent experimental data.

3.5.1. Pseudo-second order model

The pseudo-second order kinetic equation is based on the adsorption capacity of the adsorbent or solid phase. The kinetic model (Ho and McKay, 1999) is expressed as given by Eq. (3), where q_e is the amount of the AR88 adsorbed (mg/g) at equilibrium and k_2 is the equilibrium rate constant for pseudo-second order adsorption (g/mg min).

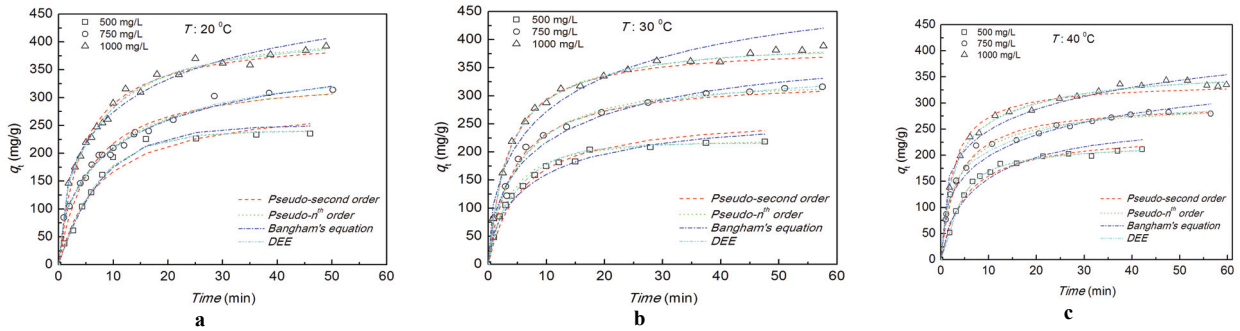

Fig. 7. Comparison of experimental and estimated adsorption kinetics of AR88 onto montmorillonitic clay as a function of time at various concentrations and temperatures. Conditions:adsorbent dosage 2 g/L, agitation speed:140 rpm, adsorption temperature:(a) 20, (b) 30 and (c) 40 °C

$$\frac{dq_t}{dt} = k_2(q_e - q_t)^2 \quad (3)$$

The initial adsorption rate, h_0 (mg/g min), as $t \rightarrow 0$ can be defined as given by Eq. (4).

$$h_0 = k_2 q_e^2 \quad (4)$$

The pseudo-second order reaction data and correlation coefficients under different temperatures were presented in Table 2 for all initial dye concentrations and at various temperatures. The values of k_2 were found to be in the ranges of 4.44×10^4 to 12.01×10^4 g/mg g for montmorillonitic clay. Further, the values of the overall second-order rate constants (k_2), increased with increase in initial AR88 concentrations from 500 mg/L to 1000 mg/L.

This increase can be explained by increase in driving force with the concentration gradient for high initial adsorbate concentration. The pseudo-second order rate constants (k_2), for adsorption of AR88 onto montmorillonitic clay indicate a steady increase with temperature. This increase can be caused from the increase in kinetic energy of dye molecules with increasing temperature. The values of rate constants were found from $5.55\text{x}10^{-4}$ to $12.01\text{x}10^{-4}$ g/mg min with an increase in the solution temperatures from 20 to 40 °C at a 1000 mg/L. It may be suggested that the adsorption of AR88 onto montmorillonitic clay follows a physisorption mechanism.

For any C_0 value in the range investigated, the initial adsorption rates (h_0) increased rapidly with increase in initial concentrations and temperatures. Estimated adsorption rates are presented in Table 2.

3.5.2. Pseudo-nth order model

The calculation of kinetic data and order of reaction is a more appropriate method than assuming the order of reaction as first or second order. The pseudo-nth order equation (Cheung et al., 2001) can be written by Eq. (5), where k_n the rate constant (g/mg min) and $\boldsymbol{n}$ is reaction order for nth-order adsorption. The surface coverage of the adsorbent is usually assumed initially to be zero (at time t=0, q_0/q_e=0). However, if the adsorbent is assumed to pre-adsorb the impurities on the surface, the surface coverage can be assumed to a certain value ($q_0/q_e \neq 0$).

$$\frac{dq_t}{dt} = k_n(q - q_t)^n \quad (5)$$

In this case, if t_0=0 and $q_0/q_e \neq 0$ the rate constant and order of reaction from kinetic data can be calculated by integrating (Eqs. 6-7) (Cheung et al., 2001)

$$q_t = q_e\left\{1 - \left[\frac{1}{\beta_n + k_n(n-1)(t-t_0)}\right]^{\frac{1}{n-1}}\right\} \quad (6)$$

$$\beta_n = 1/\left(1 - q_0/q_e\right)^{n-1} \quad (7)$$

The results indicate that the value of reaction order (n) increases with the increase in initial dye concentration and temperature (Table 2). It was found that as temperature increased, since the kinetic energy of AR88 molecules also increased, the process has occurred rapidly. In addition to this, as the temperature and initial concentration increased, when compared to the pseudo-nth order model, the reaction order ($\boldsymbol{n}$) and reaction rate constant (k_n) values increased. Tosun (2012) has obtained similar results by using the natural clinoptilolite for adsorption of ammonium.

For all initial concentrations and different temperatures, the β_n value was nearly 1. When the pre-adsorbed stage did not happen (if at time t=0, q_0/q_e=0, then β_n=1), there were no impurities or no pre-adsorbed stage on the montmorillonitic clay surface. Also, the normalized standard deviation, Δq (%) and correlation coefficients ($\boldsymbol{r^2}$) given in Table 2 indicate that the data represent pseudo nth-order model better than all other kinetic models.

3.5.3. Bangham's equation

Kinetic data were further used to know about the slow step occurring in the present adsorption system using Eq. (7) (Bangham and Burt, 1924), where: C_0 is the initial concentration of adsorbate in solution (mg/L), V is the volume of solution (mL), m is the mass of adsorbent per liter of solution (g/L), q_t is the amount of adsorbate adsorbed at time t (mg/g), and α (<1) and k_0 (mL/(g/L)) are constants.

Table 2. Values of the parameters and correlation coefficients obtained from adsorption kinetics at various initial concentrations and temperatures

C_0 (mg/L)	500			750			1000		
t (°C)	20	30	40	20	30	40	20	30	40
q_e, exp (mg/g)	235.1	218.3	211.2	313.8	313.3	286.9	390.8	388.7	335.2
Pseudo-second order									
q_e (mg/g)	295.0	266.6	243.5	341.7	330.2	298.9	413.9	389.5	340.1
$k_2 \times 10^{-4}$ (g/mg min)	4.44	6.56	7.95	5.14	7.24	9.79	5.55	7.84	12.01
h_0 (mg/g min)	38.7	46.6	47.1	60.0	79.0	87.5	95.1	118.9	138.9
r^2 (non-linear)	0.958	0.989	0.972	0.966	0.986	0.984	0.979	0.997	0.974
Δq (%)	9.3	10.4	5.1	6.6	4.6	4.1	3.6	1.7	3.5
Pseudo-nth order									
q_e, (mg/g)	240.6	222.3	217.2	324.8	320.3	311.9	416.1	409.0	397.4
n	1.006	1.529	1.716	1.431	1.463	2.400	1.611	2.161	2.913
k_n (g/mg min)	0.136	0.267	0.296	0.111	0.158	0.302	0.137	0.281	0.356
β_n	1.000	0.997	0.815	1.093	1.069	1.086	1.148	1.020	1.041
r^2 (non-linear)	0.987	0.989	0.996	0.986	0.990	0.991	0.988	0.997	0.989
Δq (%)	7.8	1.4	1.4	2.8	3.3	2.3	2.0	1.3	1.6
Bangham's equation									
k_0 (mL/(g/L))	0.063	0.127	0.107	0.119	0.132	0.140	0.135	0.128	0.160
α	0.984	0.605	0.659	0.534	0.518	0.429	0.468	0.485	0.329
r^2 (non-linear)	0.980	0.973	0.929	0.989	0.976	0.950	0.975	0.956	0.953
Δq (%)	8.9	7.2	8.6	2.8	5.0	5.0	3.0	6.7	3.8
Double exponential equation (DEE)									
q_e (mg/g)	239.8	215.3	217.4	333.5	350.1	289.1	486.4	379.9	344.4
K_{D_1} (L/min)	0.135	4.988	0.317	0.150	0.187	0.736	0.008	0.064	0.056
D_1 (mg/L)	277.7	4801.6	385.1	417.1	398.2	306.8	299.4	314.1	282.5
K_{D_2} (L/min)	0.135	0.155	0.050	0.344	0.021	0.060	0.130	0.372	0.403
D_2 (mg/L)	202.6	352.6	131.1	148.8	217.8	299.2	490.0	408.9	325.2
r^2 (non-linear)	0.987	0.992	0.996	0.991	0.991	0.977	0.990	0.998	0.990
Δq (%)	7.6	0.8	1.3	2.4	3.0	1.5	1.9	1.2	1.5

$$q_t = \frac{C_0}{m}\left(1 - \exp\left(\frac{-k_0 \times m \times t^{\alpha}}{V}\right)\right) \quad (7)$$

The plots (Fig. 7a, b and c) according to above equation did not yield perfect linear curves ($r^2 \leq 0.929$, non-linear) for AR88 removal by montmorillonitic clay showing that the diffusion of adsorbate into pores of the adsorbent is not the only rate-controlling step (Srivastava et al., 2006).

3.5.4. Double exponential equation (DEE)

The DEE accounting both with chemical and mathematical point of view was used to describe the adsorption kinetics of AR88 onto montmorillonitic clay. The model is based on a mathematical solution to describe a two step mechanism (Eq. 8) (Wilczak and Keinath, 1993), where q_e is the amount of the AR88 adsorbed (mg/g) at equilibrium, D_1 and D_2 (mg/L) are the adsorption coefficients of the rapid and the slow step, respectively. K_{D1} and K_{D2} (L/min) are the mass transfer coefficients of the rapid and slow phase, respectively.

$$q_t = q_e - \frac{D_1}{m_{ads}}\exp(-K_{D_1}t) - \frac{D_2}{m_{ads}}\exp(-K_{D_2}t) \quad (8)$$

The DEE can be considered as a diffusion model because K_{D1} and K_{D2} are the diffusion parameters controlling the overall kinetics. The rapid-step mass transfer coefficient, K_{D1} covers both external and internal diffusion, while the slow-step K_{D2} takes into account intra-particle diffusion (Weng and Pan, 2007). Table 2 lists the corresponding model fitting parameters, i.e. D_1, D_2, K_{D1} and K_{D2}. The high r^2 (all> 0.990) indicated that the data was well correlated to the DEE model, but the fitting parameters for the rapid-step and slow-step are not equal. As stated previously, the DEE model may also be used to describe the adsorption of two different sites. In this study, since the parameters D_1 and D_2 are not equal, K_{D1} and K_{D2} are not also equal, it is suggested that the process is involved with two adsorption site.

3.5.5. Comparison of adsorption kinetics

The parameter values obtained by applying kinetic models were used to estimate the variation of adsorbed-AR88 with time. The resulting curves and kinetic parameters are compared to the experimental data in Fig. 7 a-c and Table 2, respectively. As seen, the normalized standard deviation Δq (%) of the pseudo nth-order and DEE model are lower than all other models, and the correlation coefficients of these models are high.

Considering statistical parameters in Table 2, the kinetics of AR88 adsorption onto montmorillonitic clay can be described in the order of best fitting: DEE, pseudo nth-order, pseudo-second order and Bangham's equation.

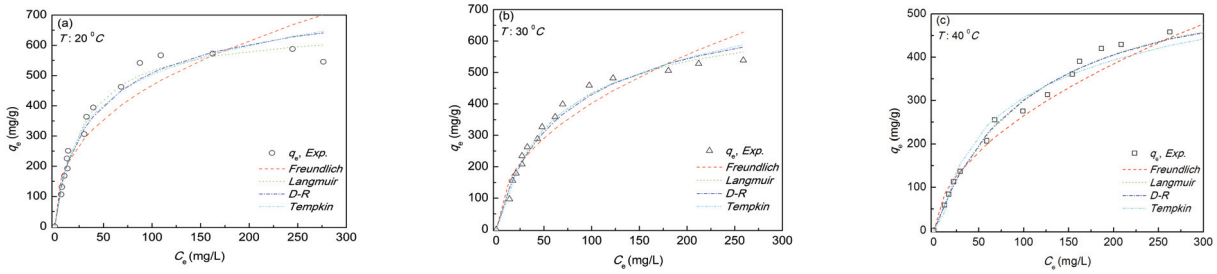

a b c

Fig. 8. Comparison of experimental and estimated adsorption isotherms of AR88 onto montmorillonitic clay at various temperatures. Conditions: C_0:150-1400 mg/L, adsorption time: 24h, adsorbent dosage 2 g/L, agitation speed: 140 rpm, adsorption temperature: (a) 20, (b) 30 and (c) 40 °C

Table 3. Values of the parameters and correlation coefficients obtained from isotherm models at various temperatures (C_0: 1400 mg/L)

Model	***Constants***	***Temperature***		
		20 °C	***30 °C***	***40 °C***
q_e, exp (mg/g)		588.0	538.8	483.8
Freundlich				
	K_F (L/g)	74.85	46.58	22.33
	1/n	0.398	0.468	0.537
	n	2.513	2.136	1.861
	r^2 (non-linear)	0.861	0.911	0.943
	Δq (%)	15.76	12.10	10.24
Langmuir				
	K_L (L/g)	23.42	11.64	5.69
	a_L (L/mg)	0.0353	0.0167	0.0090
	$q_m=K_L/a_L$ (mg/g)	662.5	695.5	631.6
	r^2 (non-linear)	0.976	0.983	0.990
	Δq (%)	6.50	5.19	4.56
Dubinin- Radushkevich				
	q_m (mg/g)	751.0	732.2	590.5
	E (kJ/mol)	6.62	5.85	5.38
	r^2 (non-linear)	0.954	0.974	0.990
	Δq (%)	9.03	6.26	4.32
Tempkin				
	K_T (L/g)	0.342	0.145	0.118
	b (J/mol)	17.17	15.03	19.59
	r^2 (non-linear)	0.953	0.981	0.980
	Δq (%)	7.60	5.02	7.27

For the range of process variables investigated, the results indicated that the adsorption kinetic coefficients are dependent on initial concentration of AR88 and temperature.

3.6. Adsorption isotherms

Adsorption isotherms are basic requirements to understand the mechanism of the adsorption. The shape of an isotherm can provide qualitative information on the nature of solution-surface interaction. In addition, adsorption isotherms are developed to evaluate the capacity of a material for the adsorption of a particular adsorbate or dye molecule (Sevim et al., 2011).

The isotherm constants, standard deviation Δq (%) and correlation coefficients (r^2) based on the actual deviation between the experimental points and predicted values are given in Fig. 8 and Table 3.

3.6.1. Freundlich isotherm

The Freundlich isotherm assumes a heterogeneous surface with a non-uniform distribution of heat of adsorption. The Freundlich isotherm is given as (Eq. 9) (Freundlich, 1906), where K_F (L/g) is related to the multilayer adsorption capacity and *n* (dimensionless) is adsorption intensity, which varies with the heterogeneity of the adsorbent.

$$q_e = K_F C_e^{1/n} \quad (9)$$

The other Freundlich constant is a measure of the deviation from linearity of the adsorption. If a value for *n* is below to unity, this implies that adsorption process is chemical, but if a value for *n* is above to unity, the process is favorable a physical adsorption. The highest value of *n* is 2.513 at 20 °C, indicates favorable adsorption at low temperature and therefore this would seem to indicate that physical

adsorption, referred the bonds become weak and conducted with van der Waals. Morris and Weber (1963) confirmed that the magnitude of *1/n* is 0.5 to be the rate-limiting step.

The Freundlich adsorption capacities, K_F, were found to be 74.85, 46.58 and 22.33 L/g at 20, 30 and 40 ºC, respectively (Table 3). However, the model was unable to describe the data due to higher standard deviation (Δq>%5).

3.6.2. Langmuir isotherm

The Langmuir isotherm theory assumes monolayer coverage of adsorbate over a homogeneous adsorbent surface. Graphically, a plateau characterizes the Langmuir isotherm. Therefore, at equilibrium, a saturation point is reached where no further adsorption can occur. Sorption is assumed to take place at specific homogeneous sites within the adsorbent. Once a dye molecule occupies a site, no further adsorption can take place at that site. In (Eq. 10), K_L (L/mg) and a_L are the Langmuir constants; C_e (mg/L) and q_e (mg/g) are the liquid phase concentration and solid phase concentration of dye at equilibrium as Eq. (10) (Allen et al., 2003; Langmuir, 1918; Pilli et al., 2010).

$$q_e = \frac{K_L C_e}{1 + a_L C_e} \tag{10}$$

The Langmuir constants, K_L and a_L are evaluated through linearization of (Eq. 10). Hence by plotting C_e/q_e against C_e it is possible to obtain the value of K_L from the intercept which is ($1/K_L$) and the value of a_L from the slope, which is (a_L/K_L). The theoretical monolayer capacity is q_m and is numerically equal to (K_L/a_L).

$$\frac{C_e}{q_e} = \frac{1}{K_L} + \frac{a_L}{K_L} C_e \tag{11}$$

Maximum monolayer adsorption capacities were 662.5, 695.5 and 631.6 mg/g for 20, 30 and 40 ^{o}C, respectively. Both the a_L and K_L values decrease with increasing temperature (Table 3).

3.6.3. Dubinin-Radushkevich (D-R) isotherm

Another equation used in the analysis of isotherms was proposed by Dubinin and Radushkevich (1960).

The D-R isotherm is applied to find out the adsorption mechanism based on the potential theory assuming heterogeneous surface. The D-R isotherm is expressed as Eq. (12), where q_m is the maximum adsorption capacity (mg/g) and the mean free energy E (kJ/mol) of adsorption was connected with D-R isotherm and calculated from (Eq. 12). The D-R parameters and activation energy are given in Table 3. The magnitude of E is useful for estimating the type of adsorption reaction. When the magnitude of E is between 8 and 16 kJ/mol, the adsorption process follows by chemical ion exchange, while for the values of E<8 kJ/mol, the kJ/mol is of a physical nature.

$$q_e = q_m \exp\left(\frac{\left(RT \ln(1 + 1/C_e)\right)^2}{-2E^2}\right) \tag{12}$$

When the temperature is increased from 20 to 40 ^{o}C, the numerical value of the mean free energy decreased from 6.62 to 5.38 kJ/mol (Table 3), which is correspond to physical nature.

3.6.4. Tempkin model

Tempkin and Pzyhev (1940) considered the effects of some indirect adsorbate-adsorbent interactions on adsorption isotherms and suggest that the heat of adsorption of all the molecules in the adsorbed layer would decrease linearly with coverage. Tempkin isotherm equation is expressed by the Eq. (13), where K_T is equilibrium binding constant (L/g), b is related to heat of adsorption (J/mol), R is the gas constant (8.314×10^{-3} kJ/K mol) and T is the absolute temperature (K).

$$q_e = \frac{RT}{b} \ln(K_T C_e) \tag{13}$$

Tempkin constants, K_T and b, were found to be 0.342, 0.145, 0.118 L/g and 17.17, 15.03, 19.59 J/mol for 20, 30 and 40 ºC, respectively. The isotherm model better described the experimental data, as it produced low standard deviation (**Δq, %**) and high regression coefficients (r^2). The Tempkin adsorption potential, K_T, decreased with increase in temperature and the constant b, related to heat of adsorption, varied between 15.03 and 19.59 J/mol (Table 3).

3.6.5. Comparison of isotherm models

Table 3 and Fig. 8 indicate that isotherm models are generally consistent with the experimental data. It was determined that best fitted adsorption isotherm models considering the relative errors were obtained in the order of prediction precision: Langmuir, D-R, Tempkin isotherms.

The standard deviation (Δq, %) of isotherms varied between 5% and 7%. However, correlation coefficients and standard deviation values, approximately 0.861-0.943 and 15.76-10.24 for Freundlich model respectively, indicate that the data are not well described by this model.

3.7. Adsorption thermodynamics

The adsorption mechanism (i.e., chemical or physical) is often an important indicator to describe the type of interactions between the adsorbent-dye molecules. If adsorption capacity decreases with increasing temperature, it may be indicative of physical and the reverse is generally true for chemisorptions (Sevim et al., 2011).

For the adsorption of AR88 onto montmorillonitic clay, the decrease in adsorption with increasing temperature and rapid adsorption kinetics, may suggest the presence of physical adsorption. Nevertheless, this case is not sufficient to determine the type of adsorption.

The type of adsorption may be determined through thermodynamic parameters such as change in Gibbs free energy (ΔG^0), enthalpy (ΔH^0), and entropy (ΔS^0) which can be determined by using Eqs. (14-16) and are given in Table 4, where K_L is the Langmuir isotherm constant, a_s is the activity of adsorbed AR88, a_e is the activity of AR88 in solution at equilibrium, v_s is the activity coefficient of the adsorbed AR88 and v_e is the activity coefficient of the AR88 in solution at equilibrium.

$$\Delta G^0 = -RT \ln K_L \quad (14)$$

$$\ln K_L = -\frac{\Delta G^0}{RT} = -\frac{\Delta H^0}{RT} + \frac{\Delta S^0}{R} \quad (15)$$

$$K_L = \frac{a_s}{a_e} = \frac{v_s q_e}{v_e C_e} \quad (16)$$

The q_e of the pseudo-second order model from Table 2 was used to obtain a_s and a_e. T is the solution temperature (K) and R is the gas constant (8.314×10^{-3} kJ/mol K). K_L can be obtained by plotting a straight line of $\ln(q_e/C_e)$ versus q_e and extrapolating q_e to zero (Fig. 9). ΔH^0 and ΔS^0 were calculated from the slope and the intercept of van't Hoff plot of $\ln K_L$ versus $10^3/T$ (see Fig. 10). The results are listed in Table 4. Generally, the change of Gibbs free energy (ΔG^0) for physisorption is between −20 and 0 kJ/mol, but chemisorptions are a range of −80 and −400 kJ/mol (Khan and Singh, 1987).

The overall ΔG^0 changes during the adsorption process were −8.38 kJ/mol at 20 °C, −7.31 kJ/mol at 30 °C, and −5.95 kJ/mol at 40 °C, which were all negative, corresponding to a spontaneous process of AR88 molecules adsorption. The negative value of the enthalpy change (ΔH^0), which is −43.90 kJ/mol, indicates that the adsorption mechanism is physical in nature involving weak forces of attraction and is also exothermic, thereby demonstrating that the process is stable energetically (Tunali et al., 2006). The negative value of the entropy change (ΔS^0), which is −121.01 J/mol K, implies that there is a decrease in the randomness in the adsorbent-solution interface and no significant changes occur in the internal structure of the adsorbent during the adsorption process (Table 4).

The pseudo-second order rate constant of dye adsorption is expressed as a function of temperature by the following Arrhenius type relationship Eq. (17) (Juang et al., 1997), where E_a (kJ/mol) is the Arrhenius activation energy of adsorption, A is the Arrhenius factor. When $\ln k_2$ is plotted versus $10^3/T$, a straight line with slope $-E_a/R$ is obtained, shown in Fig. 11.

$$\ln k_2 = \ln A - \frac{E_a}{RT} \quad (17)$$

The magnitude of activation energy gives an idea about the type of the adsorption, which is mainly physical or chemical. The values of low activation energy (5–40 kJ/mol) are characteristic of physical sorption, while values of higher activation energy (40–800 kJ/mol) suggest chemical sorption (Ozcan et al., 2006; Gu et al., 1994). The values of calculated E_a were 22.29, 24.60 and 29.41 kJ/mol for 500, 750 and 1000 mg/L initial AR88 concentration, respectively (Table 5).

Table 4. Thermodynamic parameters calculated from the Langmuir isotherm constant (K_L) for the adsorption of AR88 onto montmorillonitic clay

Temperature	K_L	*Slope*	*Intercept*	r^2	ΔG^0	ΔH^0	ΔS^0
(°C)		($\times10^{-3}$)		(linear)	(kJ/mol)	(kJ/mol)	(J/mol K)
20	31.098				−8.38		
30	18.155	5.28	−14.55	0.997	−7.31	−43.90	−121.01
40	9.832				−5.95		

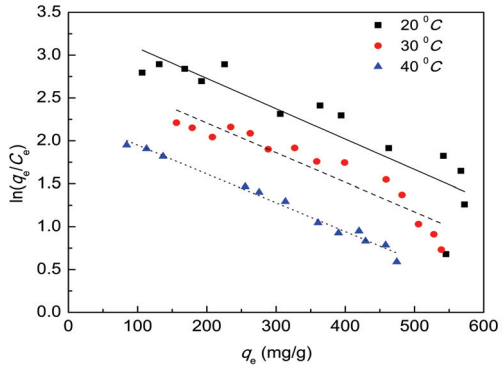

Fig. 9. Calculation of K_0 values at various temperatures

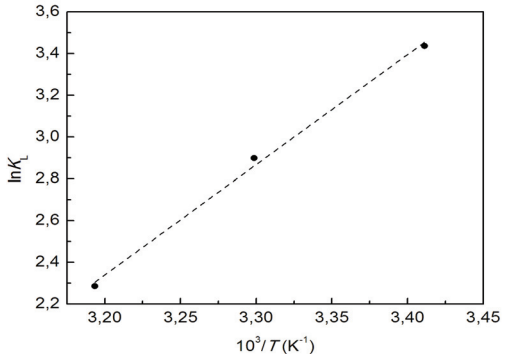

Fig. 10. Van't Hoff plot of $\ln K_L$ versus $10^3/T$ for estimation of thermodynamic parameters for the adsorption of AR88 onto montmorillonitic clay

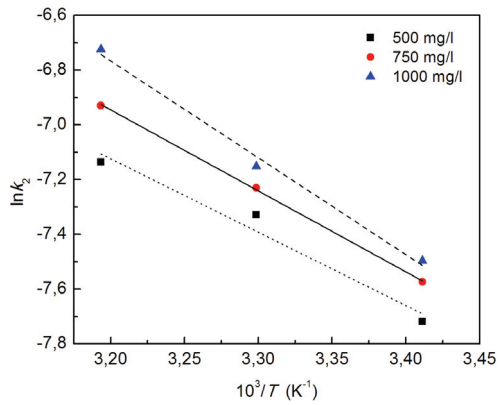

Fig. 11. Arrhenius plots of lnk_2 versus $10^3/T$ for the adsorption of AR88 onto montmorillonitic clay

The values of E_a indicate that the adsorption process has a low potential barrier and corresponding to a physical sorption mechanism. As will be mentioned in the following section, interpretation of the relationship between zeta potential and adsorption capacities supports these results.

Table 5. Arrhenius activation energies of adsorption and Arrhenius factors calculated with the pseudo-second order rate constant for AR88 onto montmorillonitic clay

Parameters	***Initial Concentration***		
	500 mg/L	***750 mg/L***	***1000 mg/L***
E_a (kJ/mol)	22.29	24.60	29.41
r^2	0.970	1.000	0.994
A	4.3	12.5	94.9

3.8. Zeta potential

It is well known from the literature that there is a relationship between adsorption of any adsorbate onto solid surface and its corresponding zeta potential (Hunter, 1988). Therefore, zeta potential has been used to explain the adsorption mechanisms of ionic surfactants, dyes, polymers, etc. (Sevim et al., 2011; Nollet et al., 2003; Zadaka et al., 2010). As illustrated in Fig. 12, there is well agreement between zeta potential curves and adsorption isotherms at 20 and 40 °C. Adsorption capacity (q_e) rapidly increased and reached ~420 mg/g at 20 °C.

In addition to this, as the AR88 was adsorbed onto montmorillonitic clay, the zeta potential of clay showed a rapid negative increase and reached -52 mV at the same equilibrium concentration. Then, when the concentration was reached to 100 mg/L, adsorbed amount reached to maximum adsorption capacity (~580 mg/g) and remained stable after this value. Similarly, zeta potential reached maximum value (–57 mV) at the same concentration.

On the other hand, as well as the increase in the amount of adsorption, zeta potential also increased and both curves remained stable after approximately 175 mg/L equilibrium concentration at 40 °C. The maximum adsorption capacity and maximum zeta potential at this temperature were approximately 420 mg/g and –60 mV, respectively. This can clearly explain the anionic dye adsorption capacity of montmorillonitic clay at natural conditions. Although the surface of montmorillonitic clay has negative charge at natural pH, the broken edges of montmorillonitic clay particles behave as the metal oxide surface and these amphoteric sites are variable in charge (either positive or negative). Depending on the pH, charges can develop at the edges by direct H^+ or OH^- transfer from aqueous phase. Thus, positive charges can occur in a protonation reaction even at basic pH (Errais et al., 2011).

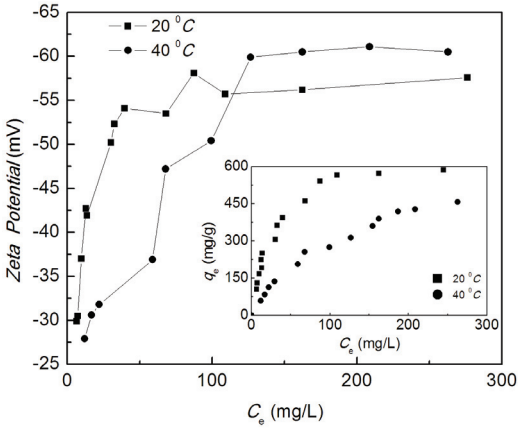

Fig. 12. The change in zeta potential with AR88 concentrations at 20 and 40 °C

3.9. The proposed adsorption mechanisms

By considering the adsorption of anionic dye (AR88) onto the montmorillonitic clay, different mechanism may be involved such as ionic attraction between anionic sulphonate group(s) of dissolved dye molecules and cationic groups of montmorillonitic clay, hydrophobic attraction of the alkyl groups.

The possible mechanisms of the adsorption of AR88 onto the clay are discussed:

I. Hydrogen bonding forces between the hydroxyl groups of AR88 and the surface silanol (–Si–OH^-) or aluminol (–Al–OH^-) or metal oxide i.e. –Si–O^- groups of clay. Actually, this is an extremely important bonding process in many clay-organic complexes. While it is less energetic than Coulombic interactions, it becomes very significant, particularly in large molecules where additive bonds of this type, coupled with a large molecular weight, may produce a relatively stable complex (Moronta, 2004). This type of bonding mechanism is also presented for various anionic dye/clay interactions (Alkan et al., 2004; Gungor and Karaoglan, 2001; Harris et al., 2001).
II. Coulombic (or electrostatic) interaction between the positively charged edge surface of clay, especially the edge surface of alumina layer and the sulfonate group(s) of AR88. As mentioned

before, the atomic structure of the edge surface of clays is entirely different from that of the basal surfaces. The charge character on the edge surface is analogous to that on the surface of silica (SiO_2) and alumina (Al_2O_3) particles. The isoelectrical point of silica is at about pH 2-3, whereas that of alumina is at about pH 9.5 (Reed, 1994; Johnson et al., 2000). The pH of the clay/dye suspension in this study was at about 8.5 under the experimental conditions. Hence, there are still some positive charges on the alumina sheets of the edge surface, which are able to attract the negatively charged dye molecules. Apart from this type of ion-ion interaction, of course, the other types of Coulombic interactions such as ion-dipole, dipole-dipole are also possible between the atoms or ions of clay surfaces and the anionic dye molecules, but they were not shown in this study.

III. Hydrophobic attraction between the non-polar segments of dye molecule i.e. benzene rings and the hydrophobic microsites on the particle surfaces i.e. siloxane (-Si-O-Si-) groups. Indeed, the clay particles are hydrophilic in character, but they also contain hydrophobic microsites at the basal surfaces, such as siloxane groups, which may interact with non-polar benzene rings. Highly hydrophobic organic pollutants, such as phenanthrene and the herbicide atrazine, have been shown to adsorb on smectites, particularly on their siloxane surface (Ozcan et al., 2006; Zadaka et al., 2010).

IV. Anion exchange between the OH^- groups linked to the metal ions at the broken surfaces and the negatively charged dyes. A similar adsorption mechanism is also proposed for adsorption of different anionic dyes (naphthol red-J and direct orange) onto nontronite at about pH 9 (Gupta et al., 2006).

V. Attractive forces in dye-dye interactions which may occur between the unadsorbed dye molecules and those adsorbed onto clay, through either a hydrogen bonding formation i.e. between their OH^- groups or hydrophobic forces controlled by van der Waals forces. It is known from the literature that these kinds of interactions can occur in adsorption of dye molecules onto adsorbents such as chitosan (Crini and Badot, 2008) and in the adsorption of other organic molecules (i.e. surfactants) on zeolite (Ersoy and Celik, 2003) and clays (Gupta et al., 2006; Xu and Boyd, 1995).

4. Conclusions

The adsorption capacity of montmorillonitic clay for AR88 was affected by various parameters such as pH, adsorbent dosage, temperature, and contact time. The following remarkable results are obtained.

- The amount of AR88 adsorbed onto montmorillonitic clay decreased with the increase in the adsorbent dosage and the optimum adsorbent dosage was found to be 2 g/L.
- FTIR results indicate that the adsorption of AR88 onto montmorillonitic clay was accomplished. There were significant differences between the vibration bands of the clay. These differences may be considered as indicator for either electrostatic interaction between the positive charges in the edge surface of montmorillonitic clay and the sulfonate groups of the anionic dye molecule or anion exchange mechanism between hydroxyl at the edge surface and anionic dye.
- The zeta potential values of the adsorbent-dye suspension increased as a result of H^+ adsorption on the surface at acidic pH values. Montmorillonitic clay did not indicate an isoelectric point since all of the zeta potential values were negative.
- The adsorption kinetics of AR88 onto montmorillonitic clay was fast, the equilibrium was attained after 30 to 60 min. The data indicated the adsorption kinetics of AR88 onto montmorillonitic clay followed the DEE and also pseudo n^{th} order model at different initial dye concentrations and temperatures.
- The isotherm models, applied to the experimental data, yielded that the most suitable model at different temperatures was the Langmuir model in terms of all obtained parameters and standard deviations. The maximum adsorption capacity was found to be 588 mg/g from Langmuir adsorption isotherm model at 20 ^oC.
- Thermodynamic quantities confirm that AR88 adsorption onto montmorillonitic clay is spontaneous, exothermic and physical in nature involving weak forces of attraction. The ΔG^0 (–8.38, –7.31, –5.95 kJ/mol, 20, 30, 40 ^oC) values were negative. Therefore, the adsorption was spontaneous and the negative value of ΔS^0 (–121.01 J/mol K) suggests a decreased randomness at the solid/water interface and no significant changes occur in the internal structure of the adsorbent during the dye adsorption process. The negative value of ΔH^0 (–43.90 kJ/mol) leads to an exothermic nature of adsorption. The calculated E_a values were 22.29, 24.60 and 29.41 kJ/mol for 500, 750, 1000 mg/L initial concentration, respectively. The positive values of E_a confirm the nature of physisorption of AR88 onto montmorillonitic clay.
- It may be concluded from above results that montmorillonitic clay can be used for uptake of textile dye from colored wastewater since it is a low-cost and abundant adsorbent.

Acknowledgements

The authors would like to thank "The Scientific and Technological Research Council of Turkey" (TUBITAK) for financially supporting this research under Contract no. 109Y163.

References

Acemioglu B., (2004), Adsorption of congo red from aqueous solution onto calcium-rich fly ash, *Journal of Colloid and Interface Science*, **274**, 371-379.

Akar T., Ozcan A.S., Tunali S., Ozcan A., (2008), Biosorption of a textile dye (acid blue 40) by cone biomass of *thuja* orientails: estimation of equilibrium, thermodynamic and kinetic parameters, *Bioresource Technology*, **99**, 3057-3065.

Akar T. S., Uysal R., (2010), Untreated clay with high adsorption capacity for effective removal of C.I. Acid Red 88 from aqueous solutions: batch and dynamic flow mode studies, *Chemical Engineering Journal*, **162**, 591-598.

Akyuz S., Akyuz T., (2006), FT-IR spectroscopic investigations of adsorption of 2-, 3- and 4-pyridinecarboxamide on montmorillonite and saponite from Anatolia, *Vibrational Spectroscopy*, **42**, 387-391.

Al-Futaisi A., Jamrah A., Al-Hanai R., (2007), Aspects of cationic dye molecule adsorption to palygorskite, *Desalination*, **214**, 327-342.

Alkan M., Demirbas O., Celikcapa S., Dogan M., (2004), Sorption of acid red 57 from aqueous solutions onto sepiolite, *Journal of Hazardous Materials*, **116**, 135–145.

Alkan M., Celikcapa S., Demirbas O., Dogan M., (2005), Removal of reactive blue 221 and acid blue 62 anionic dyes from aqueous solutions by sepiolite, *Dyes and Pigments*, **65**, 251-259.

Allen S., Gan Q., Matthews R., Johnson P.A., (2003), Comparison of optimized isotherm models for basic dye adsorption by kudzu, *Bioresource Technology*, **88**, 143–152,

Armagan B., Ozdemir O., Turan M., Celik M.S., (2003), The removal of reactive azo dyes by natural and modified sepiolites, *Biochemical Engineering Journal*, **78**, 725-732.

Banat I.M., Nigam P., Singh D., Marchant R., (1996), Microbial decolorization of textile-dye containing effluents: a review, *Bioresource Technology*, **58**, 217-227.

Bangham D.H., Burt F.P., (1924), *The Behavior of Gases in Contact with Glass Surfaces*, vol. 10, *Proceedings of the Royal Society of London. Series A, Containing Papers of a Mathematical and Physical Character*, The Royal Society Publishers, London, 481-488.

Cheung C. W., Porter J. F., Mckay, G., (2001), Sorption kinetic analysis for the removal of cadmium ions from effluents using bone char, *Water Research*, **35**, 605-612.

Chipera S.J., Bish D.L., (2002), A full-pattern quantitative analysis program for X-ray powder diffraction using measured and calculated patterns, *Journal of Applied Crystallography*, **35**, 744-749.

Colar L. A., Cocheci L., Ilinoiu E. C., Manea F., Orha C., Pode R., (2012), Adsorption of RY 125 dye from aqueous solution on a silver doped TiO_2 modified clinoptilolite, *Environmental Engineering and Management Journal*, **11**, 1375-1381.

Crini G., (2006), Non-conventional low-cost adsorbents for dye removal: a review, *Bioresource Technology*, **97**, 1061-1085.

Crini G., Badot P.M., (2008), Application of chitosan, a natural aminopolysaccharide, for dye removal from aqueous solutions by adsorption processes using batch studies: a review of recent literature, *Progress in Polymer Science*, **33**, 399-447.

Dubinin M.M., (1960), The potential theory of adsorption of gases and vapors for adsorbents with energetically non-uniform surface, *Chemical Reviews*, **60**, 235–266.

El Mouzdahir Y., Elmchaouri A., Mahboub R., Gil A., Korili S.A., (2010), Equilibrium modeling for the adsorption of methylene blue from aqueous solutions on activated clay minerals, *Desalination*, **250**, 335-338.

Eren E., (2009), Investigating of a basic dye removal from aqueous solution onto chemically modified Unye bentonite, *Journal of Hazardous Materials*, **166**, 88-93.

Eren E., Cubuk O., Ciftci H., Eren B., Caglar B., (2010), Adsorption of basic dye from aqueous solutions by modified sepiolite: equilibrium, kinetics and thermodynamics study, *Desalination*, **252**, 88-96.

Errais E., Duplay J., Darragi F., M'Rabet I., Aubert A., Huber F., Morvan G., (2011), Efficient anionic dye adsorption on natural untreated clay: kinetic study and thermodynamic parameters, *Desalination*, **275**, 74-81.

Ersoy B., Celik M.S., (2003), Effect of hydrocarbon chain length on adsorption of cationic surfactants onto clinoptilolite, *Clays and Clay Minerals*, **51**, 173-181.

Freundlich H.M.F., (1906), Over the adsorption in solution, *Journal of Physical Chemistry*, **57**, 385–470.

Fu Y., Viraraghavan T., (2002), Removal of Congo red from an aqueous solution by fungus *Aspergillus niger*, *Advances in Environmental Research*, 7, 239-247.

Ghosh D., Bhattacharyya K.G., (2002), Adsorption of methylene blue on kaolinite, *Applied Clay Science*, **20**, 295-300.

Gu B., Schmitt J., Chen Z., Liang L., McCarthy J.F., (1994), Adsorption and desorption of natural organic matter on iron oxide: mechanisms and models, *Environmental Science and Technology*, **28**, 38–46.

Gungor N., Karaoglan S., (2001), Interactions of polyacrylamide polymer with bentonite in aqueous systems, *Materials Letters*, **48**, 168-175.

Gupta V.K., Mohan D., Saini V.K., (2006), Studies on the interaction of some azo dyes (naphthol red-j and direct orange) with nontronite mineral, *Journal of Colloid and Interface Science*, **298**, 79-86.

Harris R.G., Wells J.D., Johnson B.B., (2001), Selective adsorption of dyes and other organic molecules to kaolinite and oxide surfaces, *Colloids and Surfaces A-Physicochemical and Engineering Aspects*, **180**, 131-140.

Ho Y.S. McKay G., (1999), Pseudo second-order model for sorption processes, *Process Biochemistry*, **34**, 451-465.

Hunter R.J., (1988), *Zeta Potential in Colloid Science*, Academic Press Inc., San Diego, USA.

Johnson S.B., Franks G.V., Scales P.J., Boger D.V., Healy T.W., (2000), Surface chemistry rheology relationships in concentrated mineral suspensions, *International Journal Mineral Processing*, **58**, 267-304.

Juang R.S., Wu F.C., Tseng R.L., (1997), The ability of activated clay for the adsorption of dyes from aqueous solutions, *Environmental Technology*, **18**, 525–531.

Kannan N., Sundaram M.M., (2001), Kinetics and mechanism of removal of methylene blue by adsorption on various carbons-a comparative study, *Dyes and Pigments*, **51**, 25-40.

Kapoor A., Yang R.T., (1989), Correlation of equilibrium adsorption data of condensable vapours on porous adsorbents, *Gas Separation&Purification*, **3**, 187-192.

Karaoglu M. H., Dogan M., Alkan M., (2010), Kinetic analysis of reactive blue 221 adsorption on kaolinite, *Desalination*, **256**, 154–165.

Khan A.A., Singh R.P., (1987), Adsorption thermodynamics of carbofuran on Sn (IV) arsenosilicate in H^+, Na^+ and Ca^{2+} forms, *Colloids and*

Surfaces A, **24**, 33–42.

Langmuir I., (1918), The adsorption of gases on plane surfaces of glass, mica and platinum, *Journal of the American Chemical Society*, **40**, 1361–1403.

Luis P.M.S.S., Cheng C.Y., Boaventura R.A.R., (2014), Adsorption of a basic dye onto esmegel clay, *Environmental Engineering and Management Journal*, **13**, 395-405.

Monash P., Pugazhenthi G., (2010), Removal of crystal violet dye from aqueous solution using calcined and uncalcined mixed clay adsorbents, *Separation Science and Technology*, **45**, 94-104.

Mondal P.K., Ahmad R., Kumar R., (2014), Adsorptive removal of hazardous Methylene Blue by fruit shell of *cocos nucifera*, *Environmental Engineering and Management Journal*, **13**, 231-240.

Moronta A., (2004), *Catalytic and Adsorption Properties of Modified Clay Surfaces*, In: *Clay Surfaces*, Wypych F., Satyanarayana K.G. (Eds.), Fundamentals and Applications, Elsevier Academic Press Amsterdam, 321-333.

Nollet H., Roels M., Lutgen P., Van der Meeren P., Verstraete W., (2003), Removal of PCBs from wastewater using fly ash, *Chemosphere*, **53**, 655–665.

Ogawa M., Kawai R., Kuroda K., (1996), Adsorption and aggregation of a cationic cyanine dye on smectites, *Journal of Physical Chemistry*, **100**, 16218-16221.

Ozcan A.S., Ozcan A., (2004), Adsorption of acid dyes from aqueous solutions onto acid-activated bentonite, *Journal of Colloid Interface Science*, **276**, 39-46.

Ozcan A.S., Erdem B., Ozcan A., (2005), Adsorption of acid blue 193 from aqueous solutions onto BTMA-bentonite, *Colloids and Surfaces A-Physicochemical and Engineering Aspects*, **266**, 73-81.

Ozcan A., Ozcan A.S., (2005), Adsorption of acid red 57 from aqueous solution onto surfactant-modified sepiolite, *Journal of Hazardous Materials*, **125**, 252-259.

Ozcan A., Oncu E.M., Ozcan A.S., (2006), Kinetics, isotherm and thermodynamic studies of adsorption of Acid Blue 193 from aqueous solutions onto natural sepiolite, *Colloids and Surfaces A-Physicochemical and Engineering Aspect*, **277**, 90-97.

Pilli S.R., Goud V.V., Mohanty K., (2010), Biosorption of Cr(VI) from aqueous solutions onto *hydrilla verticillata* weed: equilibrium, kinetics and thermodynamic studies, *Environmental Engineering and Management Journal*, **9**, 1715-1726.

Reed J.S., (1994), *Principles of Ceramics Processing*, 2nd Edition, John Wiley & Sons Inc. New York.

Sevim A.M., Hojiyev R., Gul A., Celik M.S., (2011), An investigation of the kinetics and thermodynamics of the adsorption of a cationic cobalt porphyrazine onto sepiolite, *Dyes and Pigments*, **88**, 25–38.

Srivastava V.C., Swamy M.M., Mall I.D., Prasad B., Mishra I.M., (2006), Adsorptive removal of phenol by bagasse fly ash and activated carbon: equilibrium, kinetics and thermodynamics, *Colloids and Surfaces A: Physicochemical and Engineering Aspects*, **272**, 89–104.

Tabak A., Eren E., Afsin B., Caglar B., (2009), Determination of adsorptive properties of a turkish sepiolite for removal of reactive blue 15 anionic dye from aqueous solutions, *Journal of Hazardous Materials*, **161**, 1087-1094.

Tehrani-Bagha A.R., Nikkar H., Mahmoodi N.M., Markazi M., Menger F.M., (2011), The sorption of cationic dyes onto kaolin: kinetic, isotherm and thermodynamic studies, *Desalination*, **266**, 274-280.

Tempkin M.I., Pyzhev V., (1940), Kinetics of ammonia synthesison promoted iron catalysts, *Acta Physico-Chimica URSS*, **12**, 327–356.

Tosun İ., (2012), Ammonium removal from aqueous solutions by clinoptilolite: determination of isotherm and thermodynamic parameters and comparison of kinetics by the double exponential model and conventional kinetic models, *International Journal of Environmental Research and Public Health*, **9**, 970-984.

Tunali S., Ozcan A.S., Ozcan A., Gedikbey T., (2006), Kinetics and equilibrium studies for the adsorption of acid red 57 from aqueous solutions onto calcined-alunite, *Journal of Hazardous Materials*, **135**, 141-148.

Tyagi B., Chudasama C., Jasra D.R.V., (2006), Determination of structural modification in acid activated montmorillonite clay by FT-IR spectroscopy, *Spectrochimica Acta A*, **64**, 273–278.

Vandevivere P.C., Bianchi R., Verstreate W., (1998), Treatment and reuse of wastewater from the textile wet processing industry: review of emerging technologies, *Journal of Chemical Technology and Biotechnology*, **72**, 289-302.

Vimonses V., Lei S., Jin B., Chow C.W.K., Saint C., (2009), Kinetic study and equilibrium isotherm analysis of congo red adsorption by clay material, *Chemical Engineering Journal*, **148**, 354-364.

Wang C.C., Juang L.C., Hsu T.C., Lee C.K., Lee J.F., Huang F.C., (2004), Adsorption of basic dyes onto montmorillonite, *Journal of Colloid Interface Science*, **273**, 80-86.

Wang Q.W., Yang Y.C., Gao H.B., (1993), *Problems on Hydrogen Bonding in Organic Chemistry*, Tianjin University Press, Tianjin.

Weber W.J., Morris C.J., (1963), Kinetics of adsorption on carbon from solution, *Journal of Sanitary Engineering Division, American Society Chemical Engineering*, **89**, 31–59.

Weng C.H., Pan Y.F., (2007), Adsorption of a cationic dye (methylene blue) onto spent activated clay, *Journal of Hazardous Materials*, **144**, 355-362.

Wilczak A., Keinath T.M., (1993), Kinetics of sorption and desorption of copper (II) and lead (II) on activated carbon, *Water Environment Research*, **65**, 238–244.

Won S.W., Choi S.B., Yun Y.S., (2006), Performance and mechanism in binding of reactive orange 16 to various types of sludge, *Biochemical Engineering Journal*, **28**, 208-214.

Xu S., Boyd S.A., (1995), Cationic surfactant sorption to vermiculitic subsoil via hydrophobic bonding, *Environmental Science&Technology*, **29**, 312-320.

Zadaka D., Radian A., Mishael Y. G., (2010), Applying zeta potential measurements to characterize the adsorption on montmorillonite of organic cations as monomers, micelles, or polymers, *Journal of Colloid and Interface Science*, **352**, 171-177.

Zaman A., Tsuchiya R., Moudgil B.M., (2002), Adsorption of a low-molecular-weight polyacrylic acid on silica, alumina, and montmorillonite, *Journal of Colloid and Interface Science*, **256**, 73-78.